Catalysis Today 151 (2010) 271–277

Contents lists available at ScienceDirect

Catalysis Today

journal homepage: www.elsevier.com/locate/cattod

Simulation of automotive NH_3 oxidation catalysts based on pre-computed rate data from mechanistic surface kinetics

M. Votsmeier [a,*], A. Scheuer [a,b], A. Drochner [b], H. Vogel [b], J. Gieshoff [a]

[a] Umicore AG & Co. KG, Rodenbacher Chaussee 4, D-63403 Hanau-Wolfgang, Germany
[b] Ernst-Berl-Institut für Technische und Makromolekulare Chemie, Technische Universität Darmstadt, D-64287 Darmstadt, Germany

ARTICLE INFO

Article history:
Available online 18 February 2010

Keywords:
Catalysis
Spline
Mapping
Mechanistic kinetics
Ammonia
Oxidation

ABSTRACT

This paper demonstrates how pre-computed rate data can be used to enable the numerically efficient implementation of mechanistic kinetics in a reactor model for an automotive ammonia slip catalyst.

In a pre-processing step the source terms for the gas species are mapped as a function of gas composition and temperature. From this map (80,000 data points), a spline interpolation function is constructed. The spline function approximates the numerical steady state solution of the kinetic model with an average error of less than 1%. Application of the rate mapping procedure results in a speedup of about two orders of magnitude.

The spline approximation is implemented in a 2-dimensional model of a monolith reactor channel that includes diffusion in the washcoat layer. Depending on the channel diameter and the washcoat thickness, diffusion limitations in the open channel and in the washcoat can have a significant influence on the NH_3 conversion. Surprisingly, the selectivity for the products N_2, N_2O and NO is not sensitive to diffusion effects in the gas phase or in the washcoat.

1. Introduction

1.1. Kinetic modeling of automotive NH_3 oxidation catalysts

In the selective catalytic reduction (SCR) process, NO_x is removed from automotive exhaust by reduction with NH_3. The challenge in this process is to achieve high NO_x conversions with minimal NH_3 breakthrough. One way to reduce NH_3 emissions is to use an NH_3-slip catalyst, which is an ammonia oxidation catalyst, frequently applied as a short zone at the outlet of the SCR catalyst. The NH_3-slip catalyst allows more aggressive ammonia dosing without increasing the NH_3 emissions.

The desired reaction in the NH_3-slip catalyst is the oxidation of NH_3 to N_2:

$$2NH_3 + 1.5O_2 \rightarrow N_2 + 3H_2O$$

Unfortunately, the production of N_2O and NO are also observed with most catalysts:

$$2NH_3 + 2O_2 \rightarrow N_2O + 3H_2O$$

$$2NH_3 + 2.5O_2 \rightarrow 2NO + 3H_2O$$

Furthermore, N_2O can be formed by the reaction of NO with NH_3:

$$2NH_3 + 2NO + 1.5O_2 \rightarrow 2N_2O + 3H_2O$$

One NH_3 oxidation catalyst that has been used for automotive applications is platinum supported on inorganic oxides. The oxidation of NH_3 on platinum is a well-studied reaction, mainly due to its importance in industrial nitric acid production. The reaction has been studied by a variety of experimental methods ranging from studies under vacuum conditions on single crystal surfaces to kinetic experiments under atmospheric pressure on polycrystalline catalyst samples. Furthermore, the energies of the reaction intermediates and the transition states have been computed by quantum mechanical methods. Micro-kinetic reaction mechanisms are available that are based on the quantum calculations and the experimental studies [1–7].

We have recently shown that the micro-kinetic models developed in the context of industrial NH_3 oxidation provide a good basis for the simulation of the automotive ammonia oxidation catalyst [8]. Despite the differences in the operating conditions (temperature, NH_3 concentration) and the catalyst (supported platinum versus platinum wires), it was shown that the existing reaction mechanisms qualitatively predict the experimentally observed conversions and product selectivities. With some minor modifications and re-parameterization, a good

* Corresponding author. Fax: +49 6181 59 4693.
E-mail address: martin.votsmeier@eu.umicore.com (M. Votsmeier).

0920-5861/$ – see front matter © 2010 Elsevier B.V. All rights reserved.
doi:10.1016/j.cattod.2010.01.018

description of the catalyst behavior under typical automotive operating conditions was achieved.

From a reactor engineering point of view, the design of the NH_3-slip catalyst is more challenging than the design of many other types of exhaust catalysts. The slip catalyst usually is implemented as a small zone at the outlet of the SCR catalyst. The requirement for low catalyst volume necessarily implies that a well-designed catalyst must operate close to the mass transfer limit. For this reason, a realistic simulation model of an ammonia slip catalyst needs to cover radial diffusion effects in the open channel and in the washcoat. In this study, this type of model is set-up as a demonstration of the rate mapping approach. The model is used to study the effects of internal and external diffusion limitations on conversion and product selectivity in an ammonia slip catalyst.

1.2. The rate mapping approach

The implementation of detailed surface reaction mechanisms in realistic reactor models is numerically demanding and, in many cases, the application of such detailed models for exhaust system design work becomes impractical due to numerical limitations. One major purpose of this paper is to demonstrate that the use of mapped pre-computed rate information provides a solution to this problem.

The coupling of detailed surface kinetics and complex reactor models requires solving the surface kinetic equations for each volume element and each time step. The standard approach is to solve the surface kinetics in a separate subroutine. This subroutine computes the steady state concentrations of the surface species for given gas phase concentrations and returns a source term for the gas species to the reactor model [9]. Due to the large number of calls, the numerical solution of the surface chemistry occupies most of the runtime of the reactor simulation. The rate mapping approach uses a pre-processing step to solve the surface chemistry for a large number of input conditions. From this pre-computed data, an interpolation function is constructed. During the runtime of the reactor simulation, the source terms for the surface mechanisms are evaluated by a numerically inexpensive call of the interpolation function.

The use of pre-computed rate information for complex reactive flow simulations is a well established technique in gas phase kinetics and is sometimes referred to as repro-modeling [10–12]. The main application areas are combustion and atmospheric chemistry [13–18]. Application of repro-modeling to gas phase kinetic systems frequently is complicated by the fact that the steady state assumption is not a good approximation. For this reason more sophisticated techniques have been developed that are based on the concept of 'intrinsic low dimensional manifolds' [19,20].

In heterogeneous catalysis the steady state approximation for the surface species generally is a valid assumption. This is exactly true for steady state simulations. Also for transient simulations the surface species can be safely assumed at steady state, if the characteristic time of accumulation is short compared to the inlet gas transients. Generally this is the case for the surface species on the precious metal. However, in exhaust gas catalysis there exist a number of storage phenomena that are slow on the timescale of the transient changes in exhaust composition. Examples are: the adsorption of NH_3 in SCR catalysts, NO_x storage in NO_x traps, oxygen storage in three way catalysts and the reversible oxidation of the platinum surface by NO_2 [21]. Of course, these transient phenomena cannot be treated as steady state. Application of the rate mapping approach to such systems requires the storage species to be explicitly treated by the mapping. This means that the surface concentration of the storage species becomes an additional input parameter of the mapping and the source terms for the storage species are represented by a separate mapping.

In principle, any interpolation technique can be applied in the repro-modeling approach; see ref. [22] for a short summary of the different techniques that have been applied in the past. In this work, we use multivariate tensor product spline functions for the interpolation of the pre-computed data. Given certain assumptions, it can be shown that a third order (cubic) spline provides the 'smoothest' interpolation of a given dataset [23].

We have previously demonstrated the applicability of the spline mapping approach for the implementation of detailed surface reaction mechanisms in reactor models using the relatively simple example of CH_4 oxidation [22]. In the present study we apply the mapping technique to the more challenging example of NH_3 oxidation in an automotive ammonia slip catalyst. NH_3 oxidation is a more challenging test case because both the overall oxidation rate and the product selectivities need to be reproduced by the spline mapping.

The application of the rate mapping approach to the kinetics of the ammonia slip catalysts is also of practical importance since – to our knowledge – no LHHW-type global kinetic models exist that describe NH_3 oxidation and the formation of the different reaction products under automotive conditions. Therefore, the application of a detailed surface mechanism in combination with the proposed mapping approach currently presents the most feasible method for treating ammonia slip catalysts in practical exhaust system simulation work.

2. Methodology

2.1. Computation of steady state reaction rates

NH_3 oxidation is described by the 10-reaction surface mechanism (Table 1) published in our previous work [8]. Reaction rates for the individual reactions are computed by Eq. (1):

$$r_k = k_{0k} \exp\left(-\frac{E_{ak}}{RT}\right) \prod_i c_i^{|\nu_{ik}|} \prod_i \theta_i^{|\nu_{ik}|} \quad (1)$$

where c_i is the concentration of gas phase species i, θ_i is the surface coverage of the surface species i and ν_{ik} is the stoichiometric coefficient of species i in reaction k. The pre-exponential factors k_{0k} and the activation energy E_{ak} of reaction k are taken from reference [8].

Source terms $\dot{s}_i$ for each gas and surface species are computed from the rates for the individual reactions (r_k) using the following formula:

$$\dot{s}_i = \sum_k \nu_{ik} r_k \quad (2)$$

The steady state coverage for the surface species are obtained by numerically integrating the following ordinary differential equation until a steady state has been reached:

$$\frac{d\theta_i}{dt} = \frac{\dot{s}}{\Gamma} \quad (3)$$

Table 1
The reaction network for ammonia oxidation. The terms "a" and "b" denote two different adsorption sites on the platinum surface: a: hollow site; b: on top site [8].

No.	Reaction	Equation
R1	NH_3 adsorption	$NH_3 + b \rightarrow NH_3 - b$
R2	NH_3 desorption	$NH_3 - b \rightarrow NH_3 + b$
R3	O_2 adsorption	$O_2 + 2a \rightarrow 2O - a$
R4	O_2 desorption	$2O - a \rightarrow O_2 + 2a$
R5	NH_3 activation	$NH_3 - b + 1.5O - a \rightarrow N - a + 1.5H_2O + 0.5a + b$
R6	NO desorption	$NO - a \rightarrow NO + a$
R7	NO adsorption	$NO + a \rightarrow NO - a$
R8	N_2 formation	$2N - a \rightarrow N_2 + 2a$
R9	NO formation	$N - a + O - a \rightarrow NO - a + a$
R10	N_2O formation	$NO - a + N - a \rightarrow N_2O + 2a$

Table 2
The input range of the mapping.

	Min	Max
T	300 K	800 K
x_{NH_3}	0.01 ppm	1000 ppm
x_{NO}	0.01 ppm	1000 ppm
x_{O_2}	2%	20%

During this integration, the gas phase concentrations and the surface temperature remain constant. The integration is carried out using the numerical solver DASSL [24].

2.2. The spline mapping procedure

The purpose of the spline mapping is to provide a fast interpolation of the source terms as a function of the gas phase concentrations and temperature. This is achieved by computing a certain number of data points and representing the functional relationship between the input parameters and the gas phase source terms by a spline function. In this work, the four input parameters are the temperature and the mole fractions of NH_3, NO and O_2. N_2O and N_2 only appear as products in the reaction mechanism and, therefore, have no influence on the reaction rates. The ranges for each of the four input parameters are listed in Table 2.

All results reported in this paper have been obtained using the scaled input parameters $1/T$, $\ln(x_{NH_3})$, $\ln(x_{NO})$ and $\ln(x_{O_2})$ during the construction and evaluation of the spline approximations. A number of preliminary numerical experiments showed that such a scaling improves the performance of the spline interpolation.

The construction of the spline functions requires input data located on a rectangular grid. In principle, the number and location of the grid points in each dimension can be chosen freely. In this work, the data points for each input dimension are evenly distributed over the input range of the scaled parameter. Twenty input points in each dimension are used for the input parameters x_{O_2}, x_{NO} and T, and 10 input points are used for the input parameter x_{O_2}. These settings provide 80,000 data points for the entire dataset.

Separate spline approximations have to be set-up for the source term of each species. In this work, these are the formation/destruction rates of NH_3, N_2O and N_2. The source term for NO can be computed from the other three source terms via the mass balance.

To achieve fast evaluation it is necessary to build the polynomials for the individual grid elements during the pre-processing phase. The coefficients of the polynomials are stored in a data table. During the runtime of the simulation, the source terms are computed by evaluating the polynomials using the tabulated coefficients. The toolbox of de Boor [23] is used for the construction and evaluation of the spline functions.

2.3. Performance measure for the spline mapping

The quality of the spline representation is determined by computing a validation test set that consists of 10,000 data points randomly sampled from the input space of the mapping.

A combination of two error criteria is used to measure the performance of the spline approximations. The first criterion is the relative error in the source terms:

$$e_i^{\mathrm{I}} = \frac{\dot{s}_{\mathrm{spline}} - \dot{s}}{\dot{s}} \tag{4}$$

where $\dot{s}$ is the source term computed by the numerical solution of Eq. (3) and $\dot{s}_{\mathrm{spline}}$ is the value obtained by the spline approximation.

If reaction rates become very small, then even large relative errors in the source term $\dot{s}$ will result in an insignificant error in the reactor output concentrations. For this reason, an estimated relative error in the output concentrations is used as a second error criterion:

$$e_i^{\mathrm{II}} = (\dot{s} - \dot{s}_{\mathrm{spline}}) \cdot \frac{\tau_{\mathrm{ref}}}{c} \tag{5}$$

where c is the inlet concentration of the respective species, and τ_{ref} is a reference reactor residence time. A value of 20 ms was used for τ_{ref}. This value is an upper limit for the expected residence time in the slip catalyst zone of an automotive SCR catalyst.

A combined error measure is computed as the sum of squares of the smaller of the two errors for each data point:

$$\hat{e} = \sqrt{\sum_1^N \frac{1}{N} (\min(e_i^{\mathrm{I}}, e_i^{\mathrm{II}}))^2} \tag{6}$$

where N is the number of test data points. In this way, calculations for fast reactions use the relative error in the source term and calculations for slow reactions use the estimated relative error in the output concentration.

The error measure is separately computed for each of the four species NH_3, N_2, N_2O and NO.

Since N_2 and N_2O are not used as input parameters for the spline mapping, the concentrations of these two species are not defined for the individual data points. For this reason, the error in the output concentration for these two species is reported relative to a reference concentration (c_{ref}) of 50 ppm:

$$e_i^{\mathrm{II}} = (\dot{s} - \dot{s}_{\mathrm{spline}}) \cdot \frac{\tau_{\mathrm{ref}}}{c_{\mathrm{ref}}} \tag{7}$$

To present a simple example: a value of 0.01 for $\hat{e}$ means that, on average, either the relative error in the source term is smaller than 1%, or the error in the outlet concentration is smaller than 0.01×50 ppm = 0.5 ppm.

2.4. Validation in a plug flow reactor model

To validate the spline mapping approach, a simple 1-dimensional isothermal plug flow reactor model was set-up.

Concentration profiles along the axial direction of the reactor are obtained by a simple explicit integration scheme:

$$\begin{aligned} &c_i(j) = c_i(j-1) + \dot{s} \cdot \Delta t \\ &\Delta t - \tau / N_{steps} \end{aligned} \tag{8}$$

where $c_i(0)$ is the inlet concentration of species i, $c_i(j)$ is the concentration after integration step j, τ is the residence time in the reactor and Δt is the timestep of the integration scheme. The source term $\dot{s}$ for the gas species is computed either by numerical solution of Eq. (3) or by evaluation of the spline function. Four-hundred timesteps ($N_{\mathrm{step}} = 400$) were used for the calculation of the results presented in this paper. It has been verified that the solution is insensitive to a further increase in the number of timesteps.

2.5. Model of a monolith channel

Finally, the spline representation of the surface reaction mechanism is implemented in an isothermal axially symmetric model of one monolith channel. This model solves the balance equations for the concentrations of the gas species in the washcoat and in the open channel.

For convection and diffusion in the gas phase of the open channel, the balance equation reads:

$$\nabla \cdot (-D_i \nabla c_i + c_i u) = 0 \tag{9}$$

where u is the axial velocity that is given by a parabolic flow profile. The gas phase diffusion coefficients of the individual species D_i are computed according to Fuller et al. [25].

The balance equation for reaction and diffusion in the washcoat is:

$$\nabla \cdot (-D_{\text{eff}} \nabla c_i) = \dot{s}_i \tag{10}$$

The source terms $\dot{s}_i$ are computed by evaluating the spline interpolation functions.

Following Zhang et al. [26], a value of $1 \cdot 10^{-6}$ m^2/s is used for the room temperature effective diffusion coefficient of all gas species in the washcoat. The temperature dependency of the effective diffusion coefficient D_{eff} is computed from the diffusion coefficient at room temperature $D_{\text{eff, RT}}$ according to:

$$D_{\text{eff}} = D_{\text{eff,RT}} \cdot \left(\frac{T}{300\,\text{K}}\right)^{1.75} \tag{11}$$

The model has been implemented in the commercial simulation package Comsol Multiphysics, Version 3.3a.

In this paper only an isothermal model of the monolith channel is solved. This is justified by the fact that the adiabatic temperature rise for the combustion of 300 pm NH_3 is less than 2.5 K. Additional implementation of the heat balance in Comsol would be straightforward.

3. Results and discussion

3.1. Performance of the rate mapping

3.1.1. Accuracy

To investigate the performance of the spline mapping, we compared the source terms predicted by different mappings to the values obtained by an exact numerical computation of the source terms. For this purpose, 10,000 data points were randomly sampled from the input domain of the mapping.

For each of the different spline representations, a combined absolute/relative average error is computed as described in Section 2.3.

Table 3 shows the average errors of different spline mappings as a function of the polynomial order of the spline. In all cases, the accuracies of the second order (quadratic) splines are significantly better than those of the linear splines. Increasing the polynomial order to three leads to a minor additional improvement. These results are in line with our previous study on methane oxidation [22]. A third order polynomial has a considerably higher number of coefficients than a second order polynomial, in our case (four input dimensions) 256 instead of 81. Therefore, the cubic spline requires significantly more storage space and processor time with little improvement in accuracy. For this reason, quadratic splines are used for the reactor simulations presented in the following sections.

Table 3
The average error as computed by Eq. (6). Splines of different orders were constructed from a dataset with $20 \times 20 \times 20 \times 10$ points. The error was computed based on a test dataset of 10,000 points that were sampled randomly from the input space given in Table 2.

	Mapped quantity	Average error		
		Linear spline	Quadratic spline	Cubic spline
NH_3	$\ln(\dot{s})$	1.89%	0.28%	0.22%
	$\dot{s}$	4.57%	1.04%	0.97%
N_2	$\ln(\dot{s})$	2.44%	0.36%	0.28%
	$\dot{s}$	9.50%	2.61%	5.01%
N_2O	$\ln(\dot{s})$	2.06%	0.26%	0.20%
	$\dot{s}$	7.71%	1.52%	2.00%
NO	Mass balance $\ln(\dot{s})$	3.53%	0.96%	0.74%
	$\dot{s}$	6.91%	1.09%	1.16%

In our previous work on methane oxidation [22], we found that a logarithmic scaling of the mapped source terms improves the accuracy of the spline approximation. Such a logarithmic scaling is possible only for those species with a fixed sign of the source term. In our study, the latter is true for NH_3 (which can be scaled as $\log(-\dot{s})$) and for N_2 and N_2O (which can be scaled as $\log(\dot{s})$).

Table 3 compares the performance of spline approximations with and without logarithmic scaling. In all cases, the logarithmic scaling improves the interpolation accuracy. The improvement is larger for the quadratic and cubic splines, where the error is reduced by a factor of about 5–10.

NO appears in the reaction mechanism as both a reactant and a product, so a logarithmic scaling is not possible in this case. In the reactor simulations, it is sufficient to compute the source terms of NH_3, N_2 and N_2O by a spline approximation. All other source terms can be computed from the mass balance.

Table 3 also reports the accuracy of an NO source term that was obtained from the mass balance. The error is comparable to the error obtained with a direct mapping of the unscaled source term of NO.

In conclusion, Table 3 shows that with an appropriate logarithmic scaling, both quadratic and cubic spline approximations compute the source terms of the relevant species (NH_3, N_2, N_2O and NO) with an average error of less than 1%. Therefore, the error introduced by the spline mapping is much lower than the expected uncertainty in the underlying surface kinetics.

3.1.2. Runtime performance

For the test set with 10,000 data points, the numerical computation of the surface rates takes 46.3 s on a dual core 2.8 GHz Intel (T9600) computer. The approximation of the three source terms for N_2, N_2O and NH_3 by the spline approximation takes 0.39 s for the 10,000 data points, corresponding to a speedup by a factor of more than 100. A comparison of the runtime performance for spline approximations of different polynomial orders is presented in Table 4.

3.2. Validation with plug flow reactor simulations

To demonstrate the performance of the rate mapping approach in reactor simulations, the spline interpolation was implemented in a simple isothermal plug flow reactor model. The results are compared to the output of the same model with direct numerical computation of the source terms. Fig. 1 shows simulation results for the oxidation of NH_3 with different NH_3 inlet concentrations. The figure displays the outlet concentrations of NH_3, N_2, N_2O and NO as a function of reactor temperature. Fig. 2 shows similar results for a reaction mixture that contains equal amounts of NO and NH_3. In all cases, the results obtained with direct numerical computation of the steady state source terms are perfectly reproduced by the rate mapping approach.

3.3. Implementation of the mapped kinetics in a 2-D simulation of a monolith channel

The mapped kinetics were implemented in a 2-dimensional model of one monolith channel. This model computes the

Table 4
A comparison of the calculation time and speedup for the spline approximations. The calculation times are for a dataset of 10,000 points. The exact numerical computation of these 10,000 data points takes 46.3 s. The computation times reported for the spline mapping include three calls of the interpolation routine for each data point (one call for each of the three source terms of NH_3, N_2 and N_2O).

	t(s)	Speedup
Linear spline	0.10	445
Quadratic spline	0.39	119
Cubic spline	1.36	34

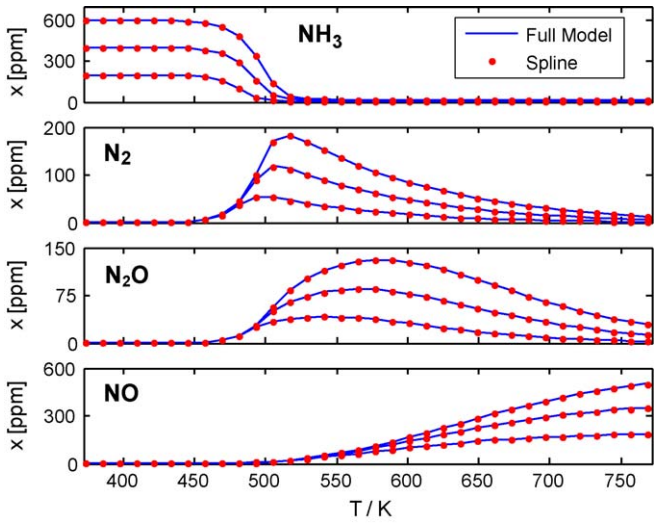

Fig. 1. Plug flow reactor simulations for three different NH_3 inlet concentrations; the concentration at reactor outlet is shown versus reactor temperature. Space velocity: 300,000 h^{-1}. Inlet concentrations: 600 ppm/400 ppm/200 ppm NH_3, 5% O_2, with no NO in the feed. Lines: full numerical solution. Dots: computation of the source term by spline interpolation.

concentration profiles in the gas phase and in the washcoat. The simultaneous treatment of mechanistic surface kinetics and washcoat diffusion effects is numerically challenging. Today, specialized simulation packages are available for this purpose [27–29]. However, these simulators require long computation times and the application of these programs seems to be limited to a few published demonstration studies. The implementation of a monolith model with detailed surface chemistry and washcoat diffusion in a commercial simulation program is even more numerically challenging than the use of the specialized solvers and, therefore, presents a good demonstration example for the rate mapping approach.

The computation of one steady state concentration profile in the 2-dimensional reactor model (1200 grid elements) takes 56 s on a 2.8 GHz Intel dual core (T9600) computer. Of the 56 s, about 30 s is spent on evaluating the spline approximations. This solution requires 674,000 computations of each of the three different source

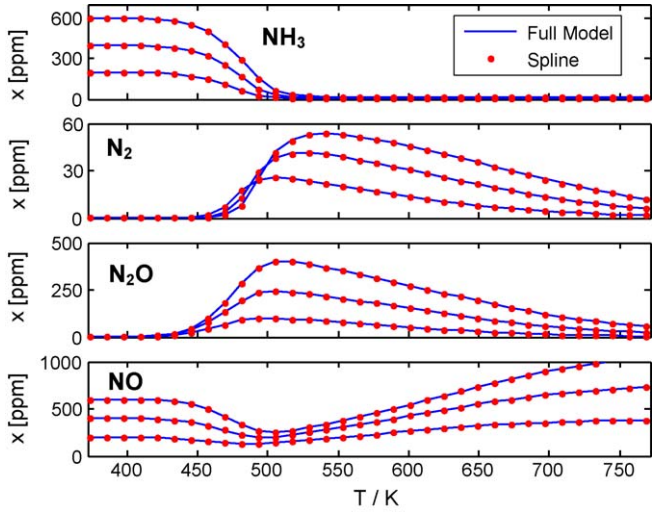

Fig. 2. Plug flow reactor simulations with equal amounts of NH_3 and NO in the feed. Space velocity: 300,000 h^{-1}. Inlet concentrations: 600 ppm/400 ppm/200 ppm NH_3/NO, 5% O_2. Lines: full numerical solution. Dots: computation of the source term by spline interpolation.

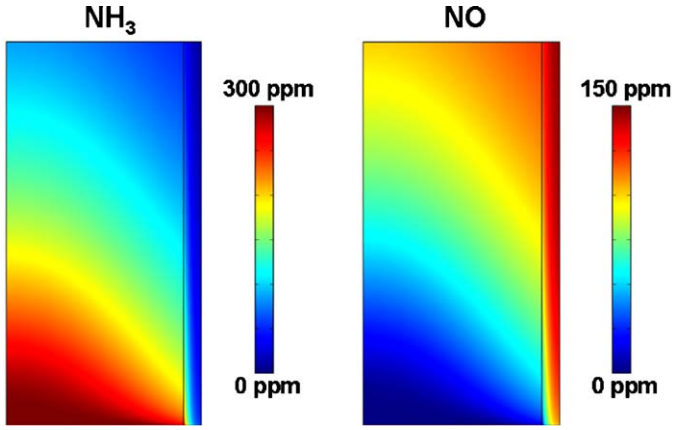

Fig. 3. Mole fraction profiles in the monolith channel. For symmetry reasons, only half of a channel is shown. The symmetry axis is on the left boundary of the model. The washcoat is in the area next to the right boundary. The flow direction is upwards. Temperature: 600 K, space velocity: 300,000 h^{-1}. Inlet concentrations: 300 ppm NH_3, 0 ppm NO, 5% O_2.

terms. Simulation with direct numerical computation of the source terms would take about 3600 s on the same computer. This results in a speed up by a factor of about 60 for the solution of the 2-D model.

Fig. 3 shows concentration profiles that were computed by the 2-D monolith reactor model for an operating temperature of 600 K. It is obvious that the NH_3 concentration shows a steep gradient in the washcoat. Such a gradient typically indicates that the reaction is diffusion-limited. Fig. 3 also shows the profile of the product NO. The highest NO concentrations are found in the washcoat. Such an accumulation of an intermediate product in the washcoat (due to diffusion limitations) can lead to an increased selectivity for secondary reaction products [30], in this case N_2O.

3.4. The effect of diffusion limitations on conversion and selectivity

To study the effect of diffusion resistance in the washcoat on overall conversion and product selectivity, simulations were performed in which the washcoat loading was varied between 5 and 200 g/L at a constant open channel diameter. In this study, the overall platinum loading of the catalyst was kept constant. This means that at higher washcoat loadings the same amount of platinum amount was distributed over a higher washcoat volume. Fig. 4 shows results of this type of washcoat loading variation for a space velocity of 300,000 h^{-1}. Increasing the washcoat loading from 5 to 25 g/L has no effect on NH_3 conversion. This result indicates that at this low washcoat loading, diffusion resistance in the washcoat can be neglected. The kinetic model used in this study has been parameterized based on experiments on a monolith with a washcoat loading of 10 g/L and it was assumed that that diffusion effects could be neglected. This assumption is supported by the simulation results shown in Fig. 4.

A further increase in the washcoat loading to 100 g/L (corresponding to a washcoat thickness of 50 μm) significantly decreases the NH_3 conversion. A loading of 200 g/L, which is a reasonable upper limit for many automotive catalyst applications, leads to a further decrease of the NH_3 conversion. At a temperature of 650 K, the NH_3 conversion is reduced to 59%, compared to 91% for the case of negligible diffusion limitation.

Surprisingly, even at the highest loadings, the washcoat thickness has no significant effect on the selectivity for N_2, N_2O and NO. Upon first inspection, this result is unexpected, since the concentration profile of Fig. 3 shows an enrichment of NO in the washcoat and our earlier experiments [8] showed a significant influence of NO on the product selectivity. A more in-depth analysis shows that the effect of NO is relevant only at lower

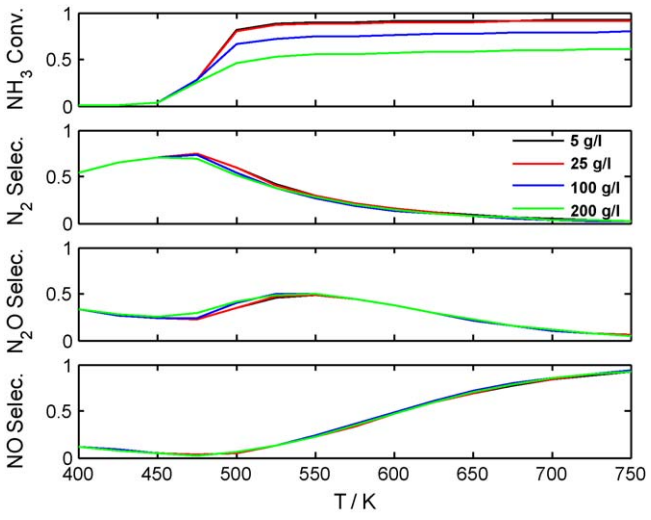

Fig. 4. Conversion and product selectivities for different washcoat loadings (at constant platinum loading). The results were computed using the 2-D model of a monolith channel. The cell density was 400 cpsi. Inlet mole fractions: 300 ppm NH_3, 0 ppm NO, 5% O_2. Hourly space velocity: 300,000 h^{-1}. Washcoat loadings: black 5 g/L, red 25 g/L, blue 100 g/L and green 200 g/L.

temperatures, where no gradient is formed in the washcoat. At higher temperatures (where the model predicts an enrichment of NO in the washcoat) the contribution of NO adsorption (reaction (7), Table 1) on the overall reaction behavior is negligible.

To analyze the effect of diffusion limitations in the gas phase, simulations have been performed for catalysts with different channel diameters. For these calculations, a very low washcoat loading of 5 g/L was used to avoid internal diffusion limitations in the washcoat. Again, the amount of precious metal loading per monolith volume was kept constant. Fig. 5 presents results for two catalysts with open channel diameters of 670 and 1400 μm, which correspond to cell densities of about 900 cpsi (cells per square inch) and 200 cpsi, respectively. The 200 cpsi catalyst shows a significant reduction in NH_3 conversion compared to the 900 cpsi catalyst. One calculation was performed, in which the radial

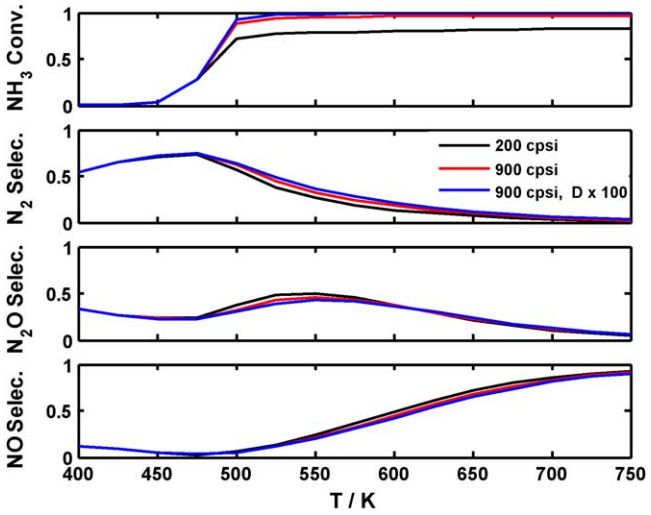

Fig. 5. The effect of external mass transfer on conversion and selectivities. The results were computed using the 2-D model of a monolith channel. The washcoat loading was 5 g/L. Inlet mole fractions: 300 ppm NH_3, 0 ppm NO, 5% O_2. Hourly space velocity: 300,000 h^{-1}. Cell density: black line: 200 cpsi and red line: 900 cpsi. In addition, one simulation was performed in which the gas phase diffusion coefficients were increased by a factor 100: blue line.

concentration gradients in the gas phase were completely avoided by multiplying the gas phase diffusion coefficients by a factor of 100. This calculation shows an insignificant increase in NH_3 conversion compared to the 900 cpsi case. This result suggests that, at least for the space velocity of 300,000 h^{-1}, a cell density of 900 cpsi is sufficient to avoid any performance degradation due to mass transfer limitations in the gas phase.

4. Conclusions

This paper demonstrates that the interpolation of pre-computed rate data by a spline function provides a numerically efficient approach for the implementation of the NH_3 oxidation surface kinetics in a monolith reactor model.

With 80,000 data points, the spline approximation reproduces the exact numerical computation of the steady state source terms with an error of less than 1%. In addition, the spline interpolation is about 2 orders of magnitude faster than the numerical solution of the kinetic rate equations.

The rate mapping approach is implemented in a 2-dimensional model of one monolith channel, taking into account the radial diffusion in the open channel and in the washcoat layer. The model is used to study the role of external and internal diffusion limitations under typical ammonia slip catalyst operation conditions. For higher washcoat loadings, diffusion resistance in the washcoat can significantly reduce NH_3 conversion. This internal diffusion limitation can be avoided if the washcoat loading is reduced to about 25 g/L. For low cell densities, ammonia conversion is also reduced by diffusion limitations in the gas phase. These external diffusion limitations become insignificant for a cell density of 900 cpsi. Neither internal nor external diffusion limitations have a significant influence on the selectivity for the products N_2, N_2O and NO.

The conclusion that diffusion limitations have to be considered for the design of ammonia slip catalysts is not unexpected. The ammonia slip catalyst is generally applied as a short zone at the outlet of the SCR catalyst and the requirement to minimize the volume of this zone implies that a well-designed ammonia slip catalyst will be operated close to the mass transfer limit.

In a previous paper, we had demonstrated the feasibility of the rate mapping approach using the relatively simple example of CH_4 oxidation. NH_3 oxidation can be considered a more challenging test case because the spline mapping needs to reproduce both the overall NH_3 conversion and the selectivity for the different reaction products. Furthermore, it has been shown that CH_4 oxidation can be described by a simple LHHW-type rate expression [31]. To our knowledge, no such global rate equations exist for the description of NH_3 oxidation and the formation of the different reaction products. On the other hand, we have recently shown [8] that existing elementary kinetics can be adopted with little effort to describe an automotive ammonia oxidation catalyst. We conclude that at the moment the application of mechanistic surface kinetics, in combination with the rate mapping technique demonstrated in this paper, presents the most practical approach for the implementation of NH_3 oxidation chemistry in simulation models that are useful for exhaust system design work.

References

[1] M. Baerns, R. Imbihl, V.A. Kondratenko, R. Kraehnert, W.K. Offermans, R.A. van Santen, A. Scheibe, Bridging the pressure and material gap in the catalytic ammonia oxidation: structural and catalytic properties of different platinum catalysts, J. Catal. 232 (2005) 226–238.

[2] R. Imbihl, A. Scheibe, Y.F. Zeng, S. Günther, R. Kraehnert, V.A. Kondratenko, M. Baerns, W.K. Offermans, A.P.J. Jansen, R.A. van Santen, Catalytic ammonia oxidation on platinum: mechanism and catalyst restructuring at high and low pressure, Phys. Chem. Chem. Phys. 9 (2007) 3522–3540.

[3] R. Kraehnert, M. Baerns, Kinetics of ammonia oxidation over Pt foil studied in a micro-structured quartz-reactor, Chem. Eng. J. 137 (2008) 361–375.
[4] G. Novell-Leruth, J.M. Ricart, J. Pérez-Ramírez, Pt(1 0 0)-catalyzed ammonia oxidation studied by DFT: mechanism and microkinetics, J. Phys. Chem. C 112 (2008) 13554–13562.
[5] W.K. Offermans, A.P.J. Jansen, R.A. van Santen, Ammonia activation on platinum {1 1 1}: a density functional theory study, Surf. Sci. 600 (2006) 1714–1734.
[6] E.V. Rebrov, M.H.J.M. de Croon, J.C. Schouten, A kinetic study of ammonia oxidation on a Pt catalyst in the explosive region in a microstructured reactor/heat-exchanger, Inst. Chem. Eng. 81 (2003) 744–752.
[7] A. Scheibe, M. Hinz, R. Imbihl, Kinetics of ammonia oxidation on stepped platinum surfaces. II. Simulation results, Surf. Sci. 576 (2005) 131–144.
[8] A. Scheuer, M. Votsmeier, A. Schuler, J. Gieshoff, A. Drochner, H. Vogel, NH3-slip catalysts: experiments versus mechanistic modelling, Top. Catal. 52 (2009) 1847–1851.
[9] O. Deutschmann, Computational fluid dynamics simulation of catalytic reactors, in: G. Ertl, H. Knözinger, F. Schüth, J. Weitkamp (Eds.), Handbook of Heterogeneous Catalysis, 2nd ed., Wiley-VCH, Weinheim, 2008, pp. 1811–1821.
[10] W.S. Meisel, D.C. Collins, Repro-modeling: an approach to efficient model utilization and interpretation, IEEE transactions on systems, man, Cybernetics 4 (1973) 349–358.
[11] T. Turanyi, Parameterization of reaction mechanisms using orthonormal polynomials, Comput. Chem. 18 (1994) 45–54.
[12] T. Turanyi, Application of repro-modelling for the reduction of combustion mechanisms, Proc. Combust. Inst. 25 (1995) 949–955.
[13] A.M. Dunker, The reduction and parameterization of chemical mechanisms for inclusion in atmospheric reaction-transport models, Atmos. Environ. 20 (1986) 479–486.
[14] S.B. Pope, Computationally efficient implementation of combustion chemistry using in situ adaptive tabulation, Combust. Theory Model. 1 (1997) 41–63.
[15] S.R. Tonse, N.W. Moriarty, N.J. Brown, M. Frenklach, PRISM: piecewise reusable implementation of solution mapping, an economical strategy for chemical kinetics, Isr. J. Chem. 39 (1999) 97–106.
[16] N. Shenvi, J.M. Geremia, H.A. Rabitz, Efficient chemical kinetic modelling through neural network maps, J. Chem. Phys. 120 (2004) 9942–9951.
[17] F.C. Christo, A.R. Masri, E.M. Nebot, Artificial neural network implementation of chemistry with pdf simulation of H-2/CO2 flames, Combust. Flame 106 (1996) 406–427.
[18] J.A. Blasco, N. Fueyo, C. Dopazo, J. Ballester, Modelling the temporal evolution of a reduced combustion chemical system with an artificial neural network, Combust. Flame 113 (1998) 38–52.
[19] U. Maas, S.B. Pope, Implementation of simplified chemical kinetics based on intrinsic low-dimensional manifolds, in: Twenty-Fourth Symposium (International) on Combustion, 1992, p. 36.
[20] A.S. Tomlin, T. Turanyi, M.J. Pilling, Mathematical tools for the construction, investigation and reduction of combustion mechanisms, in: Low-Temperature Combustion and Autoignition, ed. M.J. Pilling, Comprehensive Chemical Kinetics, vol. 35, 1997, 293–437.
[21] W. Hauptmann, M. Votsmeier, J. Gieshoff, A. Drochner, H. Vogel, Inverse hysteresis during the NO-oxidation on Pt under lean conditions, Appl. Catal. B: Environ. 93 (2009) 22–29.
[22] M. Votsmeier, Efficient implementation of detailed surface chemistry into reactor models using mapped rate data, Chem. Eng. Sci. 64 (2009) 1384–1389.
[23] C. de Boor, A Practical Guide to Splines, Springer Verlag, New York, 1978.
[24] K.E. Brenan, S.L. Campbell, L.R. Petzold, Numerical Solution of Initial-Value Problems in Differential-Algebraic Equations, Elsevier Science Publishing Co, New York, 1989.
[25] E.N. Fuller, P.D. Schettler, J.C. Giddings, New method for prediction of binary gas-phase diffusion coefficients, Ind. Eng. Chem. 58 (1966) 18–27.
[26] F. Zhang, R.E. Hayes, S.T. Kolaczkowski, A new technique to measure the effective diffusivity in a catalytic monolith washcoat, Chem. Eng. Res. Des. 82 (2000) (2004) 481–489.
[27] P. Koci, M. Kubicek, M. Marek, Modeling of three-way-catalyst monolith converters with microkinetics and diffusion in the washcoat, Ind. Eng. Chem. Res. 43 (2004) 4503–4510.
[28] O. Deutschmann, R. Schwiedernoch, L.I. Maier, D. Chatterjee, Natural gas conversion in monolithic catalysts: interaction of chemical reactions and transport phenomena, in: E. Iglesia, J.J. Spivey, T.H. Fleisch (Eds.), Natural Gas Conversion VI, 136, Studies in Surface Science and Catalysis, 2001, pp. 215–258.
[29] R. Hayes, L. Mukadi, M. Votsmeier, J. Gieshoff, Top. Catal. 30/31 (2004) 411–415.
[30] R. Aris, The Mathematical Theory of Diffusion and Reaction in Permeable Catalysts: Vol. 1—The Theory of Steady State, Clarendon Press, Oxford, 1975.
[31] S.R. Deshmukh, D.G. Vlachos, A reduced mechanism for methane and one-step rate expressions for fuel-lean catalytic combustion of small alkanes on noble metals, Combust. Flame 149 (2007) 366–383.